

Six Prism Type $\text{Ce}_{0.7}\text{La}_{0.3}\text{O}_{2-\delta}$ Solid Solution Prepared by Reverse Co-precipitation Method with Double Precipitant

HAO Hongrui^{1,a}, HAN Xue^{1, b*} and GUO Ronggui^{1,c}

¹Institute of Rare Earth Metallurgical Materials, General Research Institute for Non-Ferrous Metals, Beijing 100088, China

^ahaohongrui2012@163.com, ^bhanxuehit@126.com, ^cguorg1111@163.com

Keywords: $\text{Ce}_{1-x}\text{La}_x\text{O}_y$ solid solution; double precipitant; reverse precipitation; six prism type; $\text{Ce}_{1-x}\text{La}_x\text{O}_{2-\delta}$ (111).

Abstract. The six prism type $\text{Ce}_{0.7}\text{La}_{0.3}\text{O}_{2-\delta}$ solid solution was prepared by reverse co-precipitation method with urea and Na_2CO_3 as double precipitant. The reverse method favored the washing of precipitate and formation of rod-like CL. Using urea as a homogeneous precipitating agent before precipitation with Na_2CO_3 will help the rod-like CL turn to normal six prism. As the structure-activity relationship, uniform surface morphology will provide convenience for the catalytic reaction.

Introduction

Ceria has been extensively studied in recent years because of its wide range of potential applications in many areas of chemistry, particularly, the heterogeneous catalysis [1-5]. Ceria attracts researchers interest owing to its two important properties: (i) the redox couple, $\text{Ce}^{3+}/\text{Ce}^{4+}$ with its ability to shift between Ce_2O_3 and CeO_2 under oxidizing and reducing conditions respectively; (ii) the ease of formation of labile oxygen vacancies and oxide ion storage [6-8]. However, under elevated conditions ceria becomes inefficient with time and many innate properties will be affected [6]. Hence, ceria is commonly combined with other metal ions to make solid solutions with improved properties.

It is now well established that Zr^{4+} incorporation greatly enhances the surface area, thermal stability and oxygen storage/release capacity (OSC) of ceria, resulting in superior catalytic properties, and has been used as an important material in many catalysis application [9-15]. However, Reddy and his co-workers had systematically investigated the relative efficacies of zirconium and lanthanum in ceria solid solutions and demonstrated that compared to $\text{Ce}_{1-x}\text{Zr}_x\text{O}_2$, the $\text{Ce}_{1-x}\text{La}_x\text{O}_{2-\delta}$ solid solution (CL) sample showed a high OSC, better thermal stability and enhanced soot oxidation activity [16]. La doping greatly increased the OSC value of ceria because more oxygen vacancies were created by substitution of Ce^{4+} cations with La^{3+} cations to keep charge neutrality [17]. These newly generated defects are expected to induce more number of surface active oxygen species and improve the rate of diffusion of bulk oxygen to the surface and exchange of oxygen with the environment thereby progress in the catalytic performance [18]. The oxygen vacancies also help ceria to create a strong metal-support interaction, and promote the dispersion of noble metals [19, 20]. Comparing to pure ceria, the advantage of CL were found in many catalytic applications, for example soot oxidation [7, 21], CO oxidation [22-24], methane oxidation [25, 26], steam reforming of methane [27] and water-gas shift reaction [28-30].

We previously reported that CL supported Rh catalysts showed excellent catalytic performance for oxidative steam reforming (OSR) at low temperature and high space velocities, and the relationship among surface area, reducibility and catalytic performance was discussed in detail [17, 31]. Although urea homogeneous precipitation method is a commonly used method to prepare CL, the thermolysis of urea frequently takes a long time (more than one day). Besides, the surface morphology of the product is difficult to control, and CL with uniform microstructure was barely reported. These result in that the structure-activity relationship of CL or CL supported noble metal catalyst for the catalytic reaction was very difficult to be investigated deeply, which will inhibit the improvement of catalyst, especially for the OSR reaction. In this work, the CL was prepared by reverse co-precipitation method with double precipitant, in order to prepare a CL with uniform morphology by a easy method in a short time.

Besides, the traditional co-precipitation, reverse traditional co-precipitation and double precipitant co-precipitation methods were also used for comparison. The physicochemical properties, surface area, crystal structure and morphology of CL were investigated.

Experimental Section

Preparation. 0.07 mol cerium(III) nitrate hexahydrate ($\text{Ce}(\text{NO}_3)_3 \cdot 6\text{H}_2\text{O}$, 99%) and 0.03 mol lanthanum(III) nitrate hexahydrate ($\text{La}(\text{NO}_3)_3 \cdot 6\text{H}_2\text{O}$, 98%) were dissolved in 200 mL water. Then, 1.5 mol/L Na_2CO_3 solution (pH=11.74, 200 mL) was added into the mixed solution drop by drop with stirring. The precipitate was washed by 1 L deionized water and dried at 60 °C for 12 h, then thermally treated in a furnace at 500 °C for 5 h in air (denoted as CL-Na). Adding rare earth salt solution into Na_2CO_3 solution and keeping other condition unchanged, the product was denoted as CL-Na-R. 0.07 mol $\text{Ce}(\text{NO}_3)_3 \cdot 6\text{H}_2\text{O}$ and 0.03 mol $\text{La}(\text{NO}_3)_3 \cdot 6\text{H}_2\text{O}$ were dissolved in 200 mL water together with 0.1 mol urea, and then stirred for 1 h at 90°C. 200 mL Na_2CO_3 solution was added, and the catalysts was denoted as CL-UNa after calcination. Reversing the precipitation process and keeping other condition unchanged, the product was denoted as CL-UNa-R.

Characterization. The chemical composition of the catalyst was determined by inductively coupled plasma atomic emission spectroscopy (ICP- AES) using an OPTIMA 2000DV spectrometer. The BET (Brunauer, Emmett, and Teller) surface areas of catalysts were determined on KUBO-X 1000 high performance micro analyzer by physical adsorption measurements with N_2 at -196 °C. Prior to N_2 physical sorption, the samples were degassed at 300 °C for 3 h. X-ray powder diffraction (XRD) patterns were measured using a PANalytical X'Pert Pro diffractometer with $\text{Cu K}\alpha$ ($\lambda = 0.15406$ nm) radiation. Data of 2θ were collected from 5 to 90° or 10 to 90° with step size of 0.01°. The surface morphologies of catalysts were studied using a JSM-7001F scanning electron microscope (SEM). Prior observation, the samples were covered with thin carbon film to avoid any charge accumulation on the sample surface and to improve the image contrast. High Resolution Transmission electron microscopy (HRTEM) images were taken on a FEI Tecnai-G2-F20 microscope operated at 300 kV. Specimens were prepared by ultrasonically suspending the sample in ethanol. Droplets of the suspension were deposited on a thin carbon film supported on a standard copper grid and dried in air.

Results and Discussion

Physicochemical properties. ICP-AES analysis revealed that for all the catalysts, the bulk ratio of $\text{La}/(\text{La}+\text{Ce})$ was in the range of 30.2 ~ 30.7 mol.%, and was very close with that in precursor (Table 1). The catalysts prepared from reverse co-precipitation contained less Na^+ after washing with deionized water, which inferred that the reverse method favored washing precipitate clean. This is attributed to the improvement of precipitate settleability during the reverse precipitation.

Table 1 The precipitation process, chemical compositions, surface area and pore volume of CL catalysts.

Catalyst	Precipitant	Process	La/(La+Ce) [mol. %]	Na/(Na+La+Ce) [wt. %]	Surface area [m ² g ⁻¹]	Pore Volume [cm ³ g ⁻¹]
CL-Na	Na_2CO_3		30.2	9.6	20	0.20
CL-Na-R	Na_2CO_3	Reverse	30.6	3.8	25	0.14
CL-UNa	Urea+ Na_2CO_3		30.7	6.7	16	0.07
CL-UNa-R	Urea+ Na_2CO_3	Reverse	30.4	2.4	19	0.14

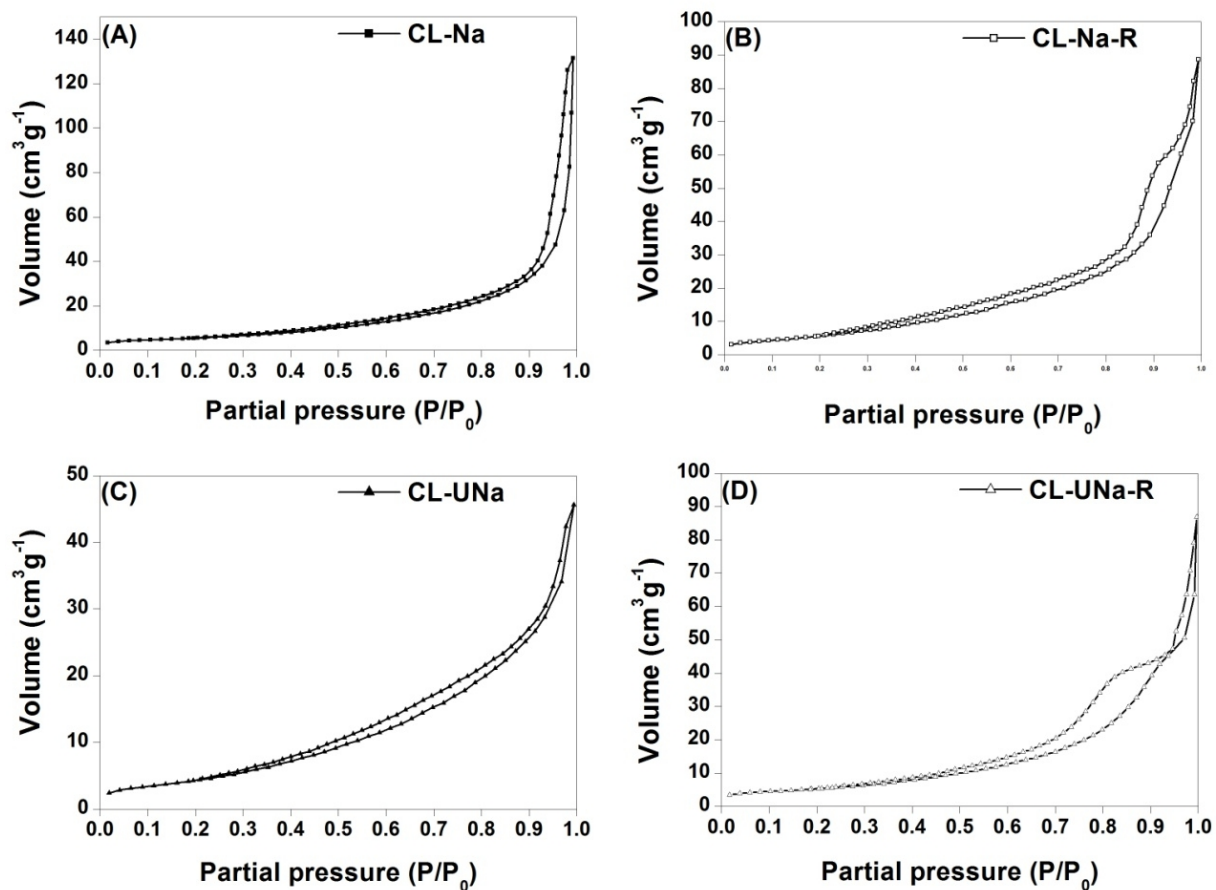


Fig. 1. Nitrogen adsorption–desorption isotherms of CL samples.

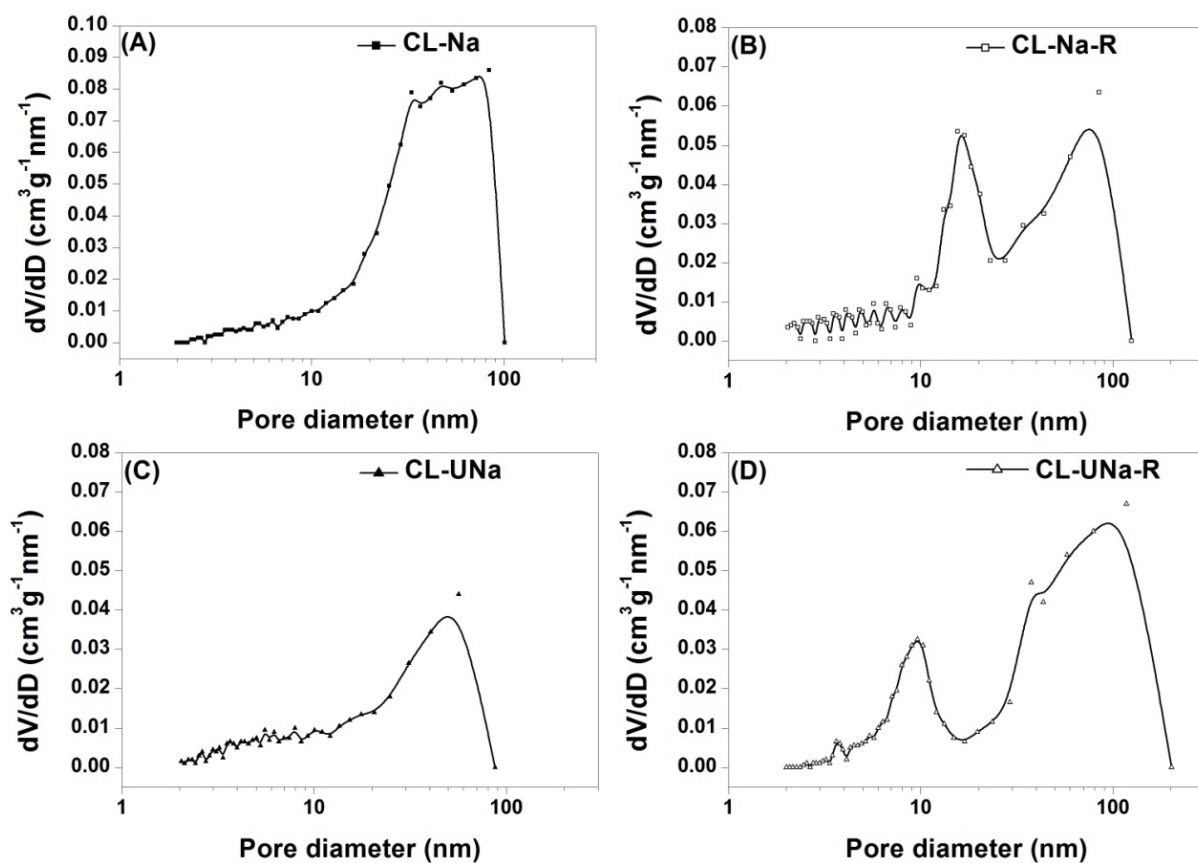


Fig. 2. Pore size distribution calculated by BJH of CL samples.

The surface area and pore volume of CL catalysts were also showed in Table 1, and these properties were not improved by introducing the reverse method and double precipitant. However, the nitrogen adsorption–desorption isotherms were changed a lot, and were summarized in Fig. 2. CL-Na and CL-UNa isotherms showed typical H3 type. These hystereses are usually found on solids consisting of aggregates or agglomerates of particles forming slit shape dpores (plates or edged particles like cubes), with nonuniform size and shape [32]. While, the catalysts prepared by reverse co-precipitation method have obviously inflection points in the desorption curve. Combining with the pore size distribution results in Fig. 3, the inflection is attributed to the two different size of pore.

Crystal structure of Catalysts. Fig. 3 presents the XRD patterns of the precipitates before calcination and CL samples. For the sample of CL-UNa before calcination, a single diffraction peak placed at $2\theta = 10^\circ$ indicates the presence of a lamellar basic nitrate; while for the CL-Na-R and CL-UNa-R samples, the incipient crystallization of a basic carbonate $\text{CeLa}(\text{OH})\text{CO}_3$ is observed [33]. All of these CL samples exhibited the characteristic diffractogram of the fluorite cubic structure of CeO_2 (JCPDS 34-0394), while no peaks due to La compounds were observed [25]. Doping of ceria with La^{3+} led to shifting of diffraction peaks toward lower angles as well as lower diffraction intensity [34]. This shift can be explained by the partial substitution of Ce^{4+} with La^{3+} , and confirmed the formation of CL solid solution.

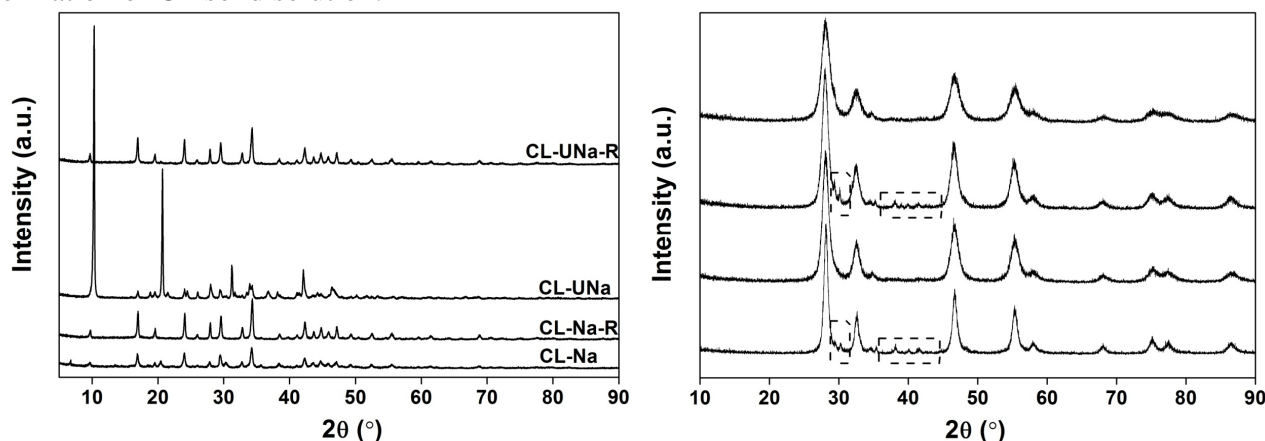


Fig.3. XRD patterns of the precipitates before calcination (left) and the CL samples (right).

Morphology of Catalysts. Fig. 4 showed SEM images of the CL samples. It is clear that the reverse method favored formation of the rod-like surface morphology. And CL-UNa-R shows a typical normal six prism type. It inferred that the introducing of the homogeneous precipitant is favored to form a CL with uniform microstructure. And the uniform large length-to-diameter ratio (>5) can explain the split peaks in pore size distribution and the inflection points in the desorption curve.

The HRTEM images of CL-Na-R and CL-UNa-R were showed in Fig. 5. CL-UNa-R sample is aggregates of ~ 8 nm solid solution particles, and show the typical $\text{Ce}_{1-x}\text{La}_x\text{O}_{2-\delta}(111)$ which was calculated by measuring interplanar spacing ($d = 0.315 \text{ \AA}$). However, for the CL-UNa sample, uniformity of the interface between particles and interplanar spacing are weaker than that of CL-UNa-R. For both of these samples, CL particles larger than 10 nm were actually agglomerates and poorly crystalline, as evidenced by the presence of Moiré fringes in many particles of size around 15 nm and above, the typical of one such was presented in Fig. 5B and Fig. 5E [35, 36].

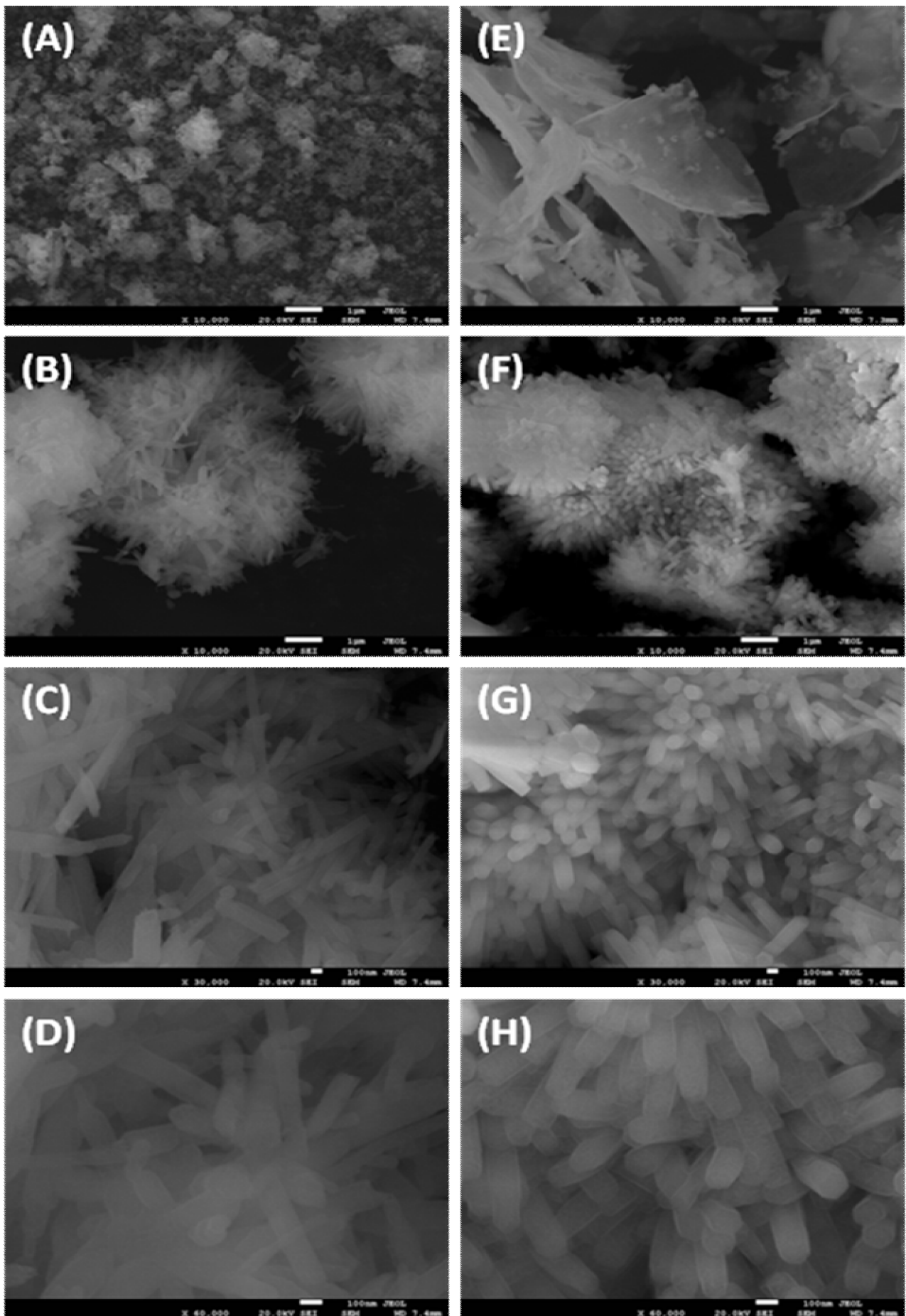


Fig. 4. SEM images of CL-Na (A), CL-Na-R (B, C, D), CL-UNa (E) and CL-UNa-R (F, G, H).

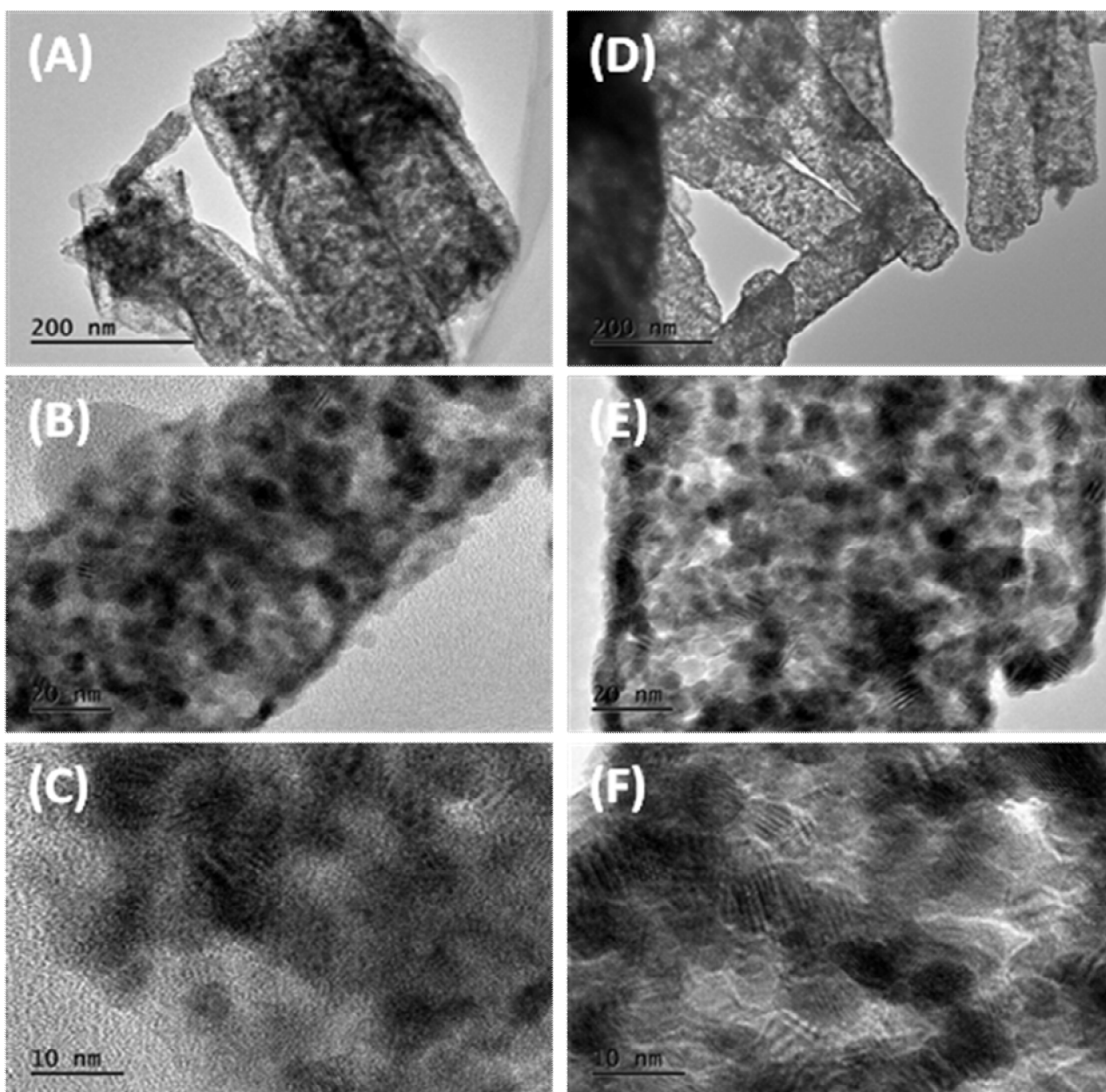


Fig. 5. HRTEM images of CL-Na-R (A, B, C) and CL-UNa-R (D, E, F).

Summary

The CL prepared by reverse co-precipitation method with double precipitant showed a uniform morphology like normal six prism. Besides, the samples prepared by traditional co-precipitation, reverse traditional co-precipitation and double precipitant co-precipitation methods were also discussed for comparison. The reverse method favored the formation of solid solution, and the Na^+ from precipitant was more easily to wash cleanly. Introducing homogeneous precipitation before the reverse co-precipitation will help the surface morphology of CL turn to a uniform normal six prism. According to the structure-activity relationship, this kind of structure is conducive to catalytic induction.

References

- [1] Y. Wei, J. Liu, Z. Zhao, A. Duan, G. Jiang, C. Xu, J. Gao, H. He, X. Wang, *Energ Environ Sci* 4 (2011) 2959-2970.

- [2] G. Zhang, Z. Zhao, J. Xu, J. Zheng, J. Liu, G. Jiang, A. Duan, H. He, *Appl Catal B* 107 (2011) 302-315.
- [3] C.Y. Ma, D.H. Wang, W.J. Xue, B.J. Dou, H.L. Wang, Z.P. Hao, *Environ Sci Technol* 45 (2011) 3628-3634.
- [4] Q.J. Xu, Y.P. Zhang, J.H. Mo, X.X. Li, *Environ Sci Technol* 45 (2011) 5754-5760.
- [5] L. Xue, H. He, C. Liu, C. Zhang, B. Zhang, *Environ Sci Technol* 43 (2009) 890-895.
- [6] B.M. Reddy, L. Katta, G. Thrimurthulu, *Chem Mater* 22 (2010) 467-475.
- [7] K. Harada, T. Oishi, S. Hamamoto, T. Ishihara, *J Phys Chem C* 118 (2014) 559-568.
- [8] M. Machida, Y. Murata, K. Kishikawa, D. Zhang, K. Ikeue, *Chem Mater* 20 (2008) 4489-4494.
- [9] Y. Wei, J. Liu, Z. Zhao, A. Duan, G. Jiang, *J Catal* 287 (2012) 13-29.
- [10] Y. Wei, J. Liu, Z. Zhao, C. Xu, A. Duan, G. Jiang, *Appl Catal A-gen* 453 (2013) 250-261.
- [11] J. Gimenez-Manogil, A. Bueno-Lopez, A. Garcia-Garcia, *Appl Catal B* 152 (2014) 99-107.
- [12] X. Wu, D. Liu, K. Li, J. Li, D. Weng, *Catal Commun* 8 (2007) 1274-1278.
- [13] S. Cai, D. Zhang, L. Zhang, L. Huang, H. Li, R. Gao, L. Shi, J. Zhang, *Catalysis Science & Technology* 4 (2014) 93-101.
- [14] Q. Wang, B. Zhao, G. Li, R. Zhou, *Environ Sci Technol* 44 (2010) 3870-3875.
- [15] G. Zhang, Z. Zhao, J. Liu, G. Jiang, A. Duan, J. Zheng, S. Chen, R. Zhou, *Chem Commun* 46 (2010) 457-459.
- [16] L. Katta, P. Sudarsanam, G. Thrimurthulu, B.M. Reddy, *Appl Catal B* 101 (2010) 101-108.
- [17] X. Han, Y. Yu, H. He, J. Zhao, Y. Wang, *J Power Sources* 238 (2013) 57-64.
- [18] L. Katta, B.M. Reddy, M. Muhler, W. Gruenert, *Catalysis Science & Technology* 2 (2012) 745-753.
- [19] J.A. Rodriguez, S. Ma, P. Liu, J. Hrbek, J. Evans, M. Pérez, *Science* 318 (2007) 1757-1760.
- [20] F.C. Meunier, D. Reid, A. Goguet, S. Shekhtman, C. Hardacre, R. Burch, W. Deng, M. Flytzani-Stephanopoulos, *J Catal* 247 (2007) 277-287.
- [21] A. Bueno-Lopez, K. Krishna, M. Makkee, J.A. Moulijn, *J Catal* 230 (2005) 237-248.
- [22] L. Katta, T.V. Kumar, D.N. Durgasri, B.M. Reddy, *Catal Today* 198 (2012) 133-139.
- [23] M.F. Wilkes, P. Hayden, A.K. Bhattacharya, *J Catal* 219 (2003) 295-304.
- [24] I. Yeriskin, M. Nolan, *J Chem Phys* 131 (2009).
- [25] B. Zhang, D. Li, X. Wang, *Catal Today* 158 (2010) 348-353.
- [26] M.F. Wilkes, P. Hayden, A.K. Bhattacharya, *J Catal* 219 (2003) 286-294.
- [27] W.H. Cassinelli, L.S.F. Feio, J.C.S. Araujo, C.E. Hori, F.B. Noronha, C.M.P. Marques, J.M.C. Bueno, *Catal Lett* 120 (2008) 86-94.
- [28] Q. Fu, W.L. Deng, H. Saltsburg, M. Flytzani-Stephanopoulos, *Appl Catal B* 56 (2005) 57-68.
- [29] Q. Fu, H. Saltsburg, M. Flytzani-Stephanopoulos, *Science* 301 (2003) 935-938.
- [30] K.C. Petalidou, A.M. Efstathiou, *Appl Catal B* 140 (2013) 333-347.
- [31] X. Han, Y. Yu, H. He, W. Shan, *Int J Hydrogen Energy* 38 (2013) 10293-10304.
- [32] L. G., P. M., T. G., V. B., *Catal Today* 41 (1998) 207-219.
- [33] M. Jobbagy, C. Sorbello, E.E. Sileo, *J Phys Chem C* 113 (2009) 10853-10857.
- [34] M.F. Wilkes, P. Hayden, A.K. Bhattacharya, *J Catal* 219 (2003) 305-309.
- [35] M. Biswas, S. Bandyopadhyay, *Mater Res Bull* 47 (2012) 544-550.
- [36] W. Cai, F. Wang, E. Zhan, A.C. Van Veen, C. Mirodatos, W. Shen, *J Catal* 257 (2008) 96-107.